JOURNAL OF GEOPHYSICAL RESEARCH, VOL. 88, NO. C9, PAGES 5203–5207, JUNE 20, 1983

Parameterization of Carbon Dioxide 15 μm Band Absorption and Emission

SZU-CHENG S. OU AND KUO-NAN LIOU

Department of Meteorology, University of Utah, Salt Lake City, Utah 84112

A parameterization scheme for carbon dioxide 15 μm band absorption and emission is developed based on the line-by-line transmittance data presented by Fels and Schwarzkopf (1981). We derive two polynomial equations to represent the broadband emissivity as functions of the temperature and pressure corrected path length. A detailed error analysis has been performed, and the root mean square errors are shown to be on the order of 5 and 7.5% for the lower and upper atmosphere cases, respectively. Cooling rates calculated from the emissivity parameterization approach show errors within about 5% when they are compared with those computed from exact line-by-line integrations.

1. INTRODUCTION

It is well known that absorption and emission of the 15 μm CO_2 band are the most significant components in the determination of terrestrial infrared cooling rates and equilibrium temperature in the stratosphere. Generally, there are three approaches to model the atmospheric infrared radiation transfer due to the 15-μm CO_2 band absorption and emission: (1) line-by-line integration over the entire band (~500–850 cm^{-1}); (2) band-by-band summation involving a limited number of sub-bands, using an approximate band model; and (3) broadband parameterization in which the absorption and emission effects are evaluated through some predetermined emissivity (or transmissivity) tables. The line-by-line approach is widely employed for the precise determination of radiative flux and cooling rate profiles. Usually, thousands of absorption lines are required in the numerical integration which takes enormous machine computation time in order to achieve reliable accuracies. The first-order approximation to the tedious and time consuming calculations is to employ an appropriate band model. The average error produced by using a band model depends on the selection of band models, the spectral resolution used, the relative importance of the Doppler broadening, and the pressure-temperature correction scheme used in estimating the effective path length over an inhomogeneous stratification [*Drayson*, 1967]. The broadband emissivity approach is a second-order approximation which utilizes a set of predetermined values. These values may be fitted by a known mathematical representation. The broadband emissivity approach is particularly useful for applications to infrared radiation energy transfer and climate modeling because of its simplicity and efficiency in numerical computations. The objective of this paper is to construct a set of broadband emissivity values for the 15-μm CO_2 band from the line-by-line data.

In the line-by-line calculation for cooling rates due to the 15-μm CO_2 band, the absorption lines can be grouped into three categories: the fundamental band, the first hot band, and the second hot band [*Dickinson*, 1973]. All these three groups include the contribution from all the isotopes. The first fundamental problem in the flux and cooling rate calculations is the assumption of local thermodynamic equilibrium (LTE) which breaks down as the altitude increases. Dickinson pointed out that a significant deviation from LTE occurs at a height around 65 km for the isotope $C^{13}O^{16}O^{18}$ and 85 km for $C^{12}O_2{}^{16}$. Thus, below about 65 km, we may safely assume LTE in radiative transfer analyses. In addition, the Doppler effect, which becomes increasingly significant to the absorption line broadening at higher altitudes, must also be taken into consideration in flux and cooling rate calculations.

Recently, *Fels and Schwarzkopf* [1981] presented an efficient algorithm using a Voigt profile for calculating carbon dioxide cooling rates based on a line-by-line computer code developed by *Drayson* [1967] which was modified to include all the hot bands and isotope contributions. They also listed 12 tables of band transmittances corresponding to two different CO_2 mixing ratios (330 and 660 ppm by volume), two different vertical resolutions (48 levels between 0 and 10 mbar as upper atmosphere resolution, and 57 levels between 0 and 1100 mbar as lower atmosphere resolution), and three different temperature profiles (one is the standard atmospheric profile and the other two are plus and minus 25°K of the standard profile). These transmittances take into account the pressure and temperature corrections in an exact manner so that no physical adjustment is required for applications to inhomogeneous atmospheres. Thus, these tables represent some of the best line-by-line data available for realistic earth atmosphere conditions at this time. We wish to utilize these fundamental data to derive a set of broadband emissivity values for the 15-μm CO_2 band for use in flux and cooling rate calculations. Since the broadband emissivity values are subject to errors, detailed error analysis is performed. Finally, cooling rates calculated from the present parameterization are compared with results published by various authors and Fels and Schwarzkopf.

2. PARAMETERIZATION

The upward and downward infrared flux at a given path length u may be written, respectively, in the form [*Liou*, 1980]

$$F^{\uparrow}(u) = \sigma T_s^4 + \int_0^u \varepsilon^f[\tilde{u} - \tilde{u}', T(u')] \frac{d\sigma T^4(u')}{du'} du' \qquad (1)$$

$$F^{\downarrow}(u) = \sigma T_1^4 \varepsilon^f(\tilde{u}_1 - \tilde{u}, T_1) + \int_{u_1}^u \varepsilon^f[\tilde{u}' - \tilde{u}, T(u')] \frac{d\sigma T^4(u')}{du'} du' \qquad (2)$$

where T_s and T_1 are the surface and top temperatures, respectively, T is the atmospheric temperature, u_1 the total

Paper number 3C0004.
0148-0227/83/003C-0004$05.00

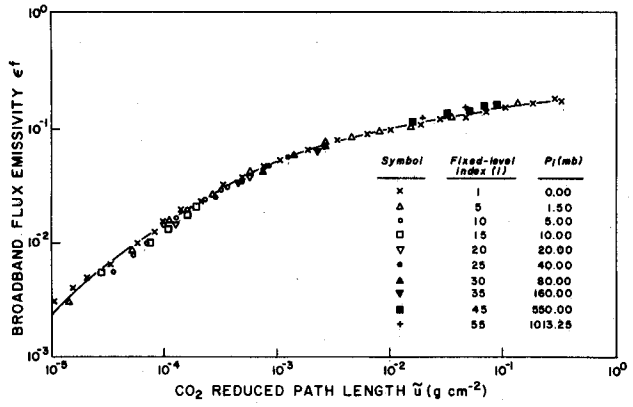

Fig. 1*a*

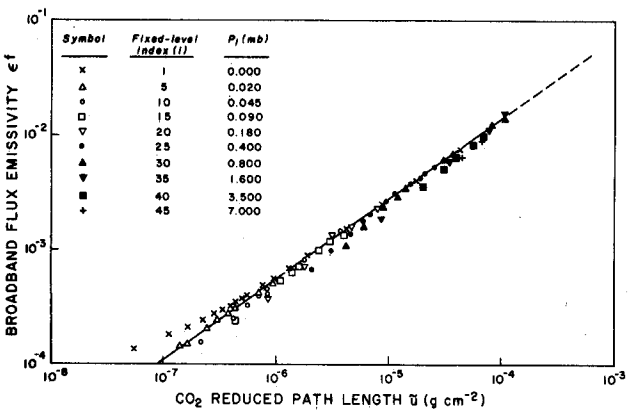

Fig. 1*b*

Fig. 1. The computed broadband flux emissivities based on the line-by-line transmission data presented by *Fels and Schwarzkopf* [1981] as functions of the temperature and pressure corrected path length $\tilde{u}$, along with the fitted curves obtained by the least square method for (*a*) the lower atmosphere and (*b*) the upper atmosphere.

path length for the absorbing gas, $\tilde{u}$ the pressure and temperature corrected path length defined below, and the broadband emissivity is defined by

$$\varepsilon^f(\tilde{u}, T) = \int_0^\infty \pi B_\nu(T)[1 - \mathrm{T}_\nu^f(\tilde{u})]\, d\nu/\sigma T^4 \qquad (3)$$

where T_ν^f is the spectral slab transmittance as defined in *Liou* [1980].

It can be shown that the transmission function, τ, defined by *Fels and Schwarzkopf* [1981], is related to the broadband emissivity as follows:

$$\varepsilon^f[\tilde{u}_i - \tilde{u}_j, T] = f(T)g(T)[1 - \tau(P_i, P_j; T_0)] \qquad (4)$$

where u_i and u_j represent path lengths for different levels P_i and P_j in the atmosphere and

$$f(T) = \frac{1 - \tau(P_i, P_j, T)}{1 - \tau(P_i, P_j, T_0)} \qquad g(T) = \frac{1}{\sigma T^4} \int_{\nu_1}^{\nu_2} \pi B_\nu(T)\, d\nu \qquad (5)$$

with $\nu_1 = 500$ cm^{-1} and $\nu_2 = 850$ cm^{-1}. In their paper, *Fels and Schwarzkopf* [1981] suggested that the temperature correction may be approximated by

$$f(T) = 1 + A\Delta T(1 - B\Delta T) \qquad (6)$$

where the constants $A = 1.833 \times 10^{-4}$, $B = 1.364 \times 10^{-2}$, and $\Delta T = T - 250$. On using (4) we may transform the tables presented by Fels and Schwarzkopf into the broadband emissivity table. However, two independent variables u_i and u_j shown in (4) need to be simplified. It was proposed by *Liou and Ou* [1981] that the broadband emissivity can be expressed as a function of a single variable $\tilde{u}$ at some reference pressure and temperature. That is, if $u = |u_i - u_j|$ and $\tilde{u} = \int_{u_i}^{u_j} \bar{P}\bar{T}\, du$, where $\bar{P} = P/P_0$ and $\bar{T} = (T_0/T)^{1/2}$, then the pressure and temperature corrected path length may be written

$$\tilde{u} = 2c/[(1 + 4y)^{1/2} - 1] \qquad y = c^2/u^2 + c/\tilde{u} \qquad (7)$$

where the constant $c = 3.7551 \times 10^{-4}$ g cm^{-2}.

To derive a unique relationship between ε^f and $\tilde{u}$, we carry out a series of computations for different path lengths by using a standard atmospheric profile. Figures 1*a* and 1*b* show the computed results for lower and upper atmospheres, respectively, using the vertical resolutions tabulated in Fels and Schwarzkopf's paper (Table 5). For $\tilde{u}$ greater than 10^{-4} g/cm^2, most of the points appear to fall on a curve except for a few small path length points. For $\tilde{u}$ smaller than 10^{-4} g/cm^2, computed points fall on a single curve for a given index i. But there is no unique curve that can fit all the points. The scatter of the points is apparently due to the Doppler effect which is not considered in the derivation of (7) and is in part due to the use of a statistical band model in deriving this equation.

On the basis of Figure 1*a*, we use a third-degree polynomial to fit the data points in the form

$$\ln \varepsilon^f = \sum_{i=0}^{3} a_i \tilde{u}'^i \qquad \tilde{u} > 10^{-4} \text{ g cm}^{-2} \qquad (8)$$

where $a_0 = -4.0089324 + \ln [f(T)g(T)/g(250)]$ $a_1 = 4.39827985$, $a_2 = -3.07709721$, and $a_3 = 0.94529227$. For the upper atmosphere shown in Figure 1*b*, we use a straight line approximation to fit the scatter points in the form

$$\ln \varepsilon^f = b_0 + b_1 \tilde{u}' \qquad \tilde{u} < 10^{-4} \text{ g cm}^{-2} \qquad (9)$$

where

$$\tilde{u}' = (2 \log \tilde{u} + 7.69897)/6.30103$$

with $b_0 = -4.00035739 + \ln [f(T)g(T)/g(250)]$ and $b_1 = 5.13453150$. At $\tilde{u} = 10^{-4}$ g cm^{-2}, values of $\ln \varepsilon^f$ calculated from (8) and (9) are, respectively, -4.226 and -4.246. Thus, there is a very slight discontinuity for the emissivity and its slope at this path length. However, we have not found any noticeable effects of this slight discontinuity on cooling rate calculations.

3. Error Analysis of the Parameterization

To examine the reliability of the curve fitting, especially for the upper atmosphere (0 ~ 10 mbar), we compute the root mean square (rms) error between the fitted curve and all the computed points. It was found that for the lower atmosphere, the rms error is about 5%, while for the upper atmosphere, it is 7.5%. The higher rms error for the upper atmosphere is largely due to the systematic scatter of data points around the fitted line at the lower end of $\tilde{u}$.

To quantify further the accuracy of the fitting based on (8) and (9), we construct two percentage error contour maps as shown in Figures 2*a* and 2*b*. In both graphs, the vertical

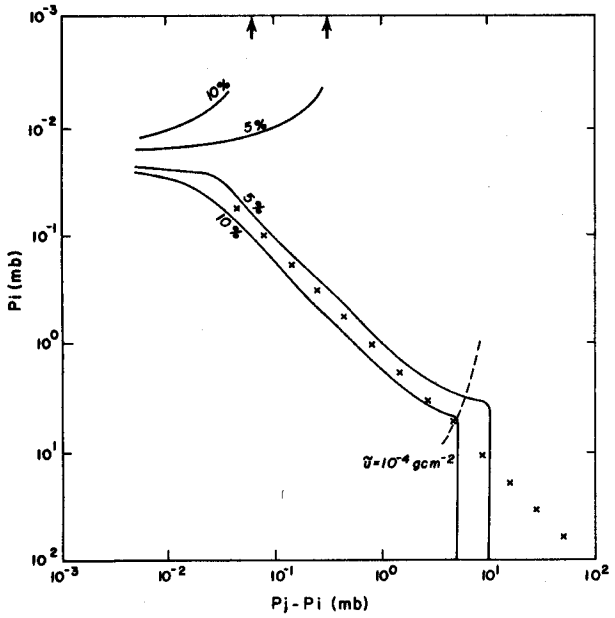

Fig. 2a

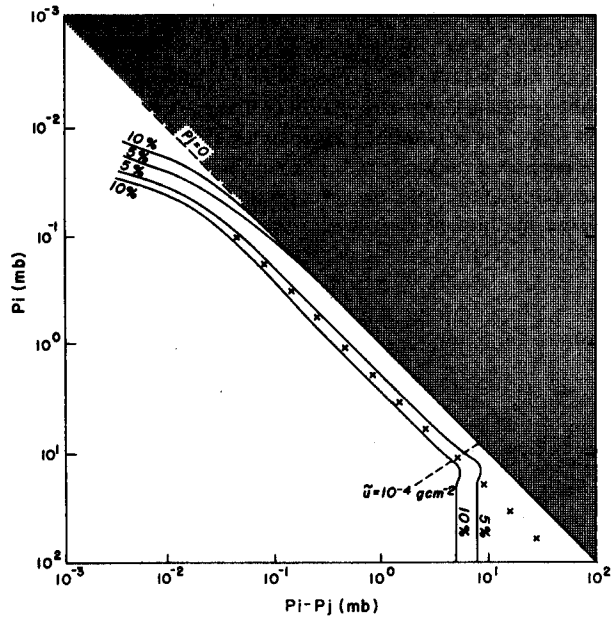

Fig. 2b

Fig. 2. Percentage error contour map showing the 5 and 10% error contour lines for the fitting shown in Figure 1; (*a*) the lower atmosphere and (*b*) the upper atmosphere. The shaded area denotes $P_j < 0$. The cross points in both graphs represent the maximum errors for each fitted level in a 32-level resolution model.

scale is the fixed-level pressure, P_i, which corresponds to the level represented by the fixed path length u in (1) and (2). The horizontal scales in Figures 2*a* and 2*b* are $P_j - P_i$ (downward pressure difference for downward flux calculations), and $P_i - P_j$ (upward pressure difference for upward flux calculations), respectively. The percentage error contour lines are constructed as follows. For each set of P_i and $P_j - P_i$ or $P_i - P_j$, an emissivity value ϵ^f can be calculated from (8) or (9). This value is then compared with that computed from the line-by-line data. The percentage error is subsequently evaluated. Thus, a set of percentage errors with respect to $(P_i, P_j - P_i)$ or $(P_i, P_i - P_j)$ can be plotted in a two-dimensional graph. The contour line with a constant error can then be constructed by drawing a curve through these points. In Figure 2*a*, where the horizontal scale is $P_j - P_i$, the 5 and 10% contour lines are seen to be largely parallel. The area to the right of either line represents that the percentage error of the emissivity value determined from the fitted equation is less than that denoted by that line, while the area to the left of the contour line corresponds to a larger error. In the area between $P_i = 1.5 \times 10^{-2}$ mbar and $P_i = 2.3 \times 10^{-2}$ mbar, the associated emissivity error is particularly low because the line-by-line points fall very close to the fitted line (see Figure 1*a*). The dashed line in the lower right part of the graph represents a combination of P_i and $P_i - P_j$ which will give a corrected path length of 10^{-4} g/cm^2. In the area to the right and below the dashed line, the error is largely dependent on $P_j - P_i$ since the error contour lines are perpendicular to the abscissa.

In Figure 2*b*, the shaded area, representing $P_i - P_j > P_i$ (or $P_j < 0$), is physically and computationally inapplicable. It is noted that the lower part of this graph shows a similar behavior as in Figure 2*a*. However, roughly above $P_i = 0.1$ mbar, the region, representing errors lower than 5 or 10%, is narrowed into a band. In addition, the region above 10^{-2} mbar is invariably associated with errors greater than 10%. It is evident that larger errors will restrict the applicability of the emissivity fitting below a certain pressure level. For example, if the error is to be limited within 10%, the fitting can only be applied to the pressure level greater than 0.05 mbar (~70 km), and the minimum pressure difference involved in the numerical integration must be greater than 0.015 mbar.

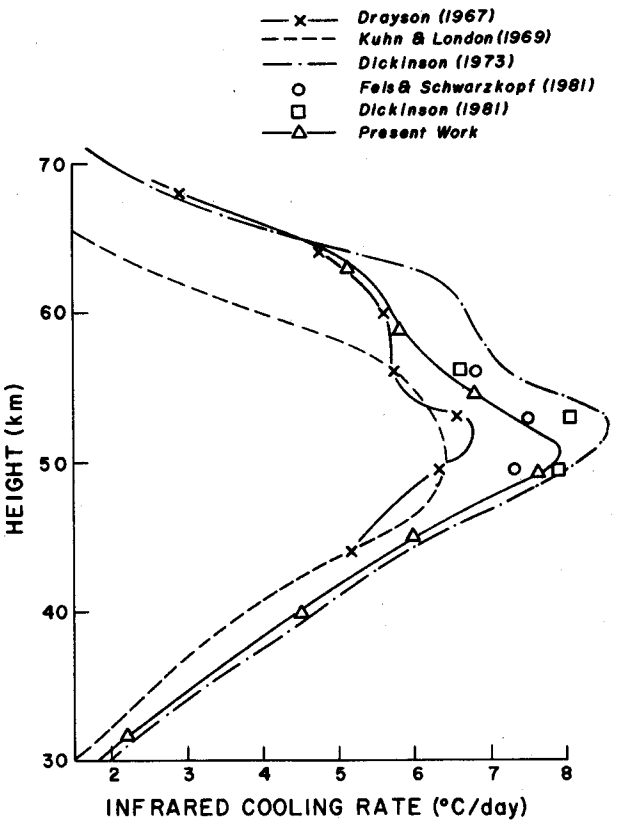

Fig. 3. Comparison of the infrared cooling rates due to the 15 μm CO_2 band obtained from the present parameterization scheme and those from published results for a standard atmosphere.

TABLE 1. Comparisons of the CO_2 Cooling Rate Obtained From the Present Study With Other Published Results Along With the Basic Parameters Used in Each Source

	Present	Drayson	Kuhn and London	Dickinson	Fels and Schwarzkopf	Dickinson
Atmospheric profile	standard	standard	standard	standard	standard	standard
CO_2 mixing ratio (ppm)	330	314	300	330	330	330
Fundamental band	yes	yes	yes	yes	yes	yes
Isotope band	yes	yes	yes	yes	yes	yes
First hot band	yes	yes	yes	yes	yes	yes
Second hot band	yes	no	no	yes	yes	yes
Doppler broadening	yes	yes	yes	yes	yes	yes
Method used	p*	l†	l	l	l	l
Cooling rates at						
49.5 km	7.6	6.3	6.4	8.0	7.36	7.84
53 km	7.3	6.5	6.2	8.5	7.49	8.01
56 km	6.5	5.7	5.7	7.2	6.82	6.62

*p = parameterization.
†l = line-by-line calculation.

In the numerical computations of the upward and downward fluxes according to (1) and (2), the integrals are approximated by summations based on the trapezoidal rule in the form

$$\int \varepsilon^f \frac{d(\sigma T^4)}{du'} du' \approx \sum_j \varepsilon_j^f \Delta_j(\sigma T^4) \tag{10}$$

where Δ_j is the finite difference operator defined as $\Delta_j(x) = x_{j+1} - x_j$. Assuming that the emissivity errors are fixed at $r\%$, i.e.,

$$\tilde{\varepsilon}_j^f = \varepsilon_j^f(1 + 0.01\, r) \tag{11}$$

where $\tilde{\varepsilon}_j^f$ and ε_j^f are the emissivity values evaluated based on fitted equations and line-by-line data, respectively. Substituting (11) into (10) we find

$$\sum_j \tilde{\varepsilon}_j^f \Delta_j(\sigma T^4) = (1 + 0.01\, r) \sum_j \varepsilon_j^f \Delta_j(\sigma T^4) \tag{12}$$

Consequently, the resulting flux as well as flux divergence will also exhibit $r\%$ error.

To examine the relationship between the cooling rate and emissivity errors in a realistic atmosphere, we use a 32-level resolution of a standard atmospheric profile. The upper 16 levels are equally divided in the logarithm of the pressure scale between 8 and 70 km. This division takes into account both the requirement of pressure differences and the necessity of adequate vertical levels to cover the temperature field. Maximum emissivity errors associated with this resolution for each fixed level P_i are illustrated both in Figures 2*a* and 2*b*. It is seen that these errors are very close to the 5% error contour line. Thus, we anticipate that the resulting flux and cooling rate errors should be limited within about 5%.

In Figure 3, infrared cooling rates due to the 15 μm CO_2 band are shown, utilizing the present emissivity parameterization scheme. Also included in the figure are a number of published results given by *Drayson* [1967], *Kuhn and London* [1969], *Dickinson* [1973], *Fels and Schwarzkopf* [1981], and *Dickinson* [1981, as cited by Fels and Schwarzkopf]. The important features considered and the actual cooling rates derived from these studies are listed in Table 1. From these comparisons, it is noted that the present results differ from those of *Fels and Schwarzkopf* [1981] by no more than 0.3°C/day ($\lesssim$5%). On inspection of the results presented in Table 1 and Figure 3, we find that cooling rates computed by *Drayson* [1967] and *Kuhn and London* [1969] are less than those reported by *Dickinson* [1973] and *Fels and Schwarzkopf* [1981]. It is evident that this is due to the neglect of the second hot band by the former authors and probably also due in part to the smaller CO_2 mixing ratio used in their calculations. The contribution of the second hot band to the cooling rate is generally greater than 1°C/day in the 45–60 km height range [*Dickinson*, 1973]. All the foregoing comparisons were for a standard atmospheric temperature profile. We have also carried out comparisons of the CO_2 cooling rates calculated from the present parameterization method and the method of *Fels and Schwarzkopf* [1981] utilizing a polar temperature profile depicted in Figure 1 of their paper. The latter results were kindly provided to us by Mr. Schwarzkopf through a private communication. Comparison results demonstrated in Figure 4 reveal that two cooling rate

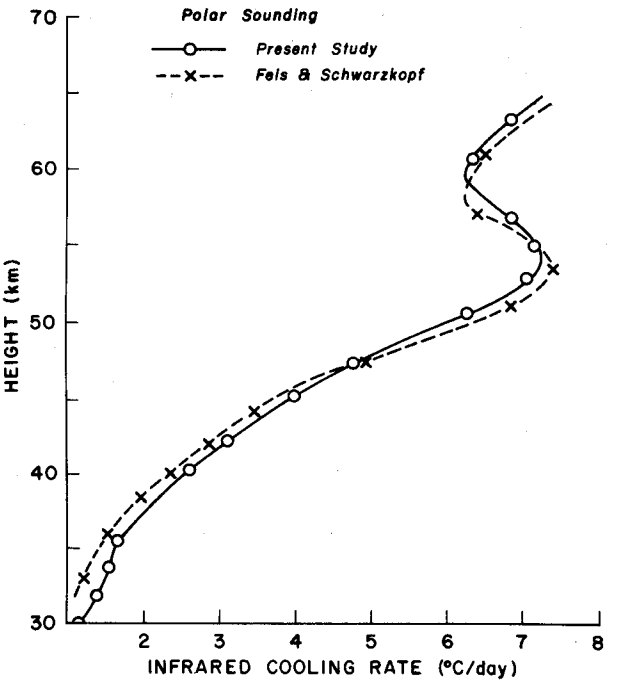

Fig. 4. Comparison of the infrared cooling rates due to the 15 μm CO_2 band obtained from the present parameterization scheme and that from the method of *Fels and Schwarzkopf* [1981] for a polar temperature profile depicted in Figure 1 of their paper.

profiles agree reasonably well with a maximum difference of about 0.5°C/day which is within about 5% error range denoted previously. We note that above 50 km cooling is much more pronounced in the polar atmosphere because of warmer temperatures in that region when compared with the standard temperature profile. In a recent review paper, *Ramanathan and Coakley* [1978] gave a detailed discussion on errors in the computations of atmospheric thermal structure caused by the uncertainties in cooling rate results. They conclude that a 5% total cooling rate error could cause a temperature error of about 3°K in the region around 40 km. According to their discussion, this temperature error is considered to be acceptable in the radiative-convective model.

4. CONCLUSION

A parameterization scheme for carbon dioxide 15 μm band absorption and emission is developed based on the line-by-line transmittance data presented by *Fels and Schwarzkopf* [1981]. Two polynomial equations for broadband emissivities are derived by means of a least square method. The root mean square errors for the fittings are shown to be on the order of 5 and 7.5% for lower and upper atmospheres, respectively. An error analysis reveals that most of the error occurs near the lower end of the pathlength range. Using a low-resolution profile, e.g., a 32-level resolution based on an equal division of pressure in the logarithmic scale, the maximum error is limited within about 5% or so. Comparisons of carbon dioxide cooling rates derived from the present parameterization scheme with those presented by Fels and Schwarzkopf show deviations are within about 0.5°C/day.

In the present parameterization we show that it is possible to reduce the cooling rate error to about 5% by using a broadband emissivity approach by properly selecting the vertical resolution. The present parameterization scheme is very efficient and computationally economic and should prove to be useful for applications to dynamic and climate models.

Acknowledgments. Research was supported by the Division of Atmospheric Sciences of the National Science Foundation under grant ATM 81-09050 and by the Air Force Geophysics Laboratory under contract F19628-81-K-0042. We thank M. D. Schwarzkopf for providing us the cooling rates for a polar temperature profile depicted in Figure 4 and Sharon Bennett for typing and editing the manuscript.

REFERENCES

Dickinson, R. E., Method of parameterization for infrared cooling between altitudes of 30 and 70 kilometers, *J. Geophys. Res., 78,* 4451–4457, 1973.

Drayson, S. R., Calculation of long-wave radiative transfer in planetary atmospheres, Ph.D. dissertation, *Rep. 07584-1-T,* 110 pp., College of Eng., Univ. of Mich., Ann Arbor, 1967.

Fels, S. B., and M. D. Schwarzkopf, An efficient, accurate algorithm for calculating CO_2 15 μm band cooling rates, *J. Geophys. Res., 86,* 1205–1232, 1981.

Kuhn, W. R., and J. London, Infrared radiative cooling in the middle atmosphere, *J. Atmos. Sci., 26,* 189–204, 1969.

Liou, K. N., *An Introduction to Atmospheric Radiation,* Academic, New York, 1980.

Liou, K. N., and S. S. Ou, Parameterization of infrared radiative transfer in cloudy atmospheres, *J. Atmos. Sci., 38,* 2707–2716, 1981.

Ramanathan, V., and J. A. Coakley, Climate modeling through radiative-convective models, *Rev. Geophys. Space Phys., 16,* 465–489, 1978.

(Received September 7, 1982;
revised December 20, 1982;
accepted December 28, 1982.)